



## Sensorless-BLDC motor speed control with ensemble Kalman filter and neural network

Muhammad Rif'an<sup>a,\*</sup>, Feri Yusivar<sup>b</sup>, Benyamin Kusumoputro<sup>b</sup>

<sup>a</sup> Department of Electrical Engineering, Universitas Negeri Jakarta  
Rawamangun Muka, Jakarta, 13220, Indonesia

<sup>b</sup> Department of Electrical Engineering, Universitas Indonesia  
Kampus Baru UI, Depok, 16424, Indonesia

Received 6 August 2018; accepted 14 March 2019; Published online 17 December 2019

### Abstract

The use of sensorless technology at BLDC is mainly to improve operational reliability and play a role for wider use of BLDC motors in the future. This research aims to predict load changes and to improve the accuracy of estimation results of sensorless-BLDC. In this paper, a new filtering algorithm is proposed for sensorless brushless DC motor based on ensemble Kalman filter (EnKF) and neural network. The proposed EnKF algorithm is used to estimate speed and rotor position, while neural network is used to estimate the disturbance by simulation. The proposed algorithm requires only the terminal voltage and the current of three phases for estimated speed and disturbance. A model of non-linear systems is carried out for simulation. Variations in disturbances such as external mechanical loads are given for testing the performance of the proposed algorithm. The experimental results show that the proposed algorithm has sufficient control with error speed of 3 % in a disturbance of 50 % of the rated-torque. Simulation results show that the speed can be tracked and adjusted accordingly either by disturbances or the presence of disturbances.

©2019 Research Centre for Electrical Power and Mechatronics - Indonesian Institute of Sciences. This is an open access article under the CC BY-NC-SA license (<https://creativecommons.org/licenses/by-nc-sa/4.0/>).

Keywords: ensemble Kalman filter; neural network; sensorless; brushless DC motor.

### 1. Introduction

Brushless DC (BLDC) Motor is a direct current motor which is electronically controlled because it does not use a brush. Currently, BLDC motors have been global utilization in many manufacturing because of their superior peculiarities, like big starting torque, great efficiency, low noise during function and high ability to withstand wear, pressure, or damage. These advantages have made BLDC motor to be widely used in electric vehicles, computers (hard disks, fans) and medical equipment [1][2][3]. The electric commutator on BLDC motor uses an inverter and assists the position sensor to catch the position of the rotor as a reference for proper current change. This is done in the line of the commutator function and the use of brushes on DC motors. The BLDC rotor rotation is a representation of the rotor position measured by the position sensor (usually using a hall sensor) and generally uses three hall sensors to get a

perfect rotation. However, the installation of the hall sensor causes several problems when adding sensors that can reduce the reliability and robustness of the system, difficult installation and maintenance, and increase the physical size and overall costs [4].

To overcome this problem, in recent years, many researchers have focused on sensorless BLDC controls. The use of sensorless technology at BLDC is mainly to improve operational reliability and play a role for wider use of BLDC motors in the future. One method that is widely used in sensorless techniques is back-EMF. In principle, this method detects back-EMF BLDCM and is used as a commutation point in accordance with the liaison between back-EMF and rotor position. Many Back-EMF methods have been developed such as the third harmonic from back-EMF sensing [5][6], back-EMF integration [7], line to line voltage sensing [8][9], filtering phase [10][11] and terminal voltage sensing [12][13]. However, all of these methods have problems at low speeds because the back-EMF amplitude is too small to be detected. The other sensorless method is Flux Calculation Method [14], but it also has problem of accumulating

\* Corresponding Author. Tel: +62 815 8165 545  
E-mail: m.rifan@unj.ac.id

integration errors at low speeds, as the previously proposed method. This method also requires considerably computing costs and is susceptible to parameter variations, so this complicated algorithm requires costly floating point processors. Another sensorless method developed by researchers is the use of observer functions. Meanwhile, a popular type of observer used to approximate the BLDC rotor position is the extended Kalman filter (EKF) [15]. However, this method has several disadvantages, including complicated calculations from the Jacobian matrix, only first order-accuracy, etc. To cover the drawback of the EKF algorithm, especially in the use of Jacobian matrix, EnKF algorithm has been developed [16]. In predicting rotor position, the EnKF algorithm no longer uses Jacobian matrix but uses ensemble integration method or better known as the Monte Carlo algorithm. Meanwhile, the prediction of mathematical problem used in the EnKF algorithm is Fokker-Planck mathematical problem. Related applications of EnKF have been reported in [16] where the use of observers as predictors of the BLDC rotor position, a mathematical model from BLDC is needed. However, the BLDC motor drive has a non-linear nature so that it is quite difficult to get accurate mathematical models for motors by using conventional techniques. In addition, with increasing usage period and difficulty in calculating non-linear parameters, motor properties are often unknown to the changes in load, disturbance, point of saturation, and BLDC parameters.

Unlike [16] which has not included fluctuation in load on the BLDC, this paper uses neural network algorithm to predict load changes based on current changes that occur in the BLDC and is used in the EnKF algorithm to improve the accuracy of estimation results. The neural network is used because of its ability to model nonlinear systems. The research was conducted by simulation of algorithm calculation using MATLAB. Simulation results show that the speed can be tracked and adjusted accordingly either by disturbances or the presence of disturbances.

## II. Materials and Methods

### A. Mathematical model of the BLDC in sensorless mode

The BLDC motor is modelled by approaching two main numerical conditions. One numerical condition is for electricity and the other one is for mechanical parts. The specifics of numerical conditions are given in [15]. Four state variables in these equations are motor shaft speed and motor current, i.e.  $i_a$ ,  $i_b$ , and  $i_c$ . The motor's mechanical, electrical, and load equations are combined as a matrix form as follows:

$$\frac{d}{dt} \begin{bmatrix} i_a \\ i_b \\ i_c \\ \omega \end{bmatrix} = \begin{bmatrix} A11 & 0 & 0 & A14 \\ 0 & A22 & 0 & A24 \\ 0 & 0 & A33 & A34 \\ A41 & A42 & A43 & A44 \end{bmatrix} \begin{bmatrix} i_a \\ i_b \\ i_c \\ \omega \end{bmatrix} + \begin{bmatrix} B11 & 0 & 0 & 0 \\ 0 & B22 & 0 & 0 \\ 0 & 0 & B33 & 0 \\ 0 & 0 & 0 & B44 \end{bmatrix} \begin{bmatrix} v_a \\ v_b \\ v_c \\ T_m \end{bmatrix} \quad (1)$$

with

$$\begin{aligned} A11 &= A22 = A33 = \frac{-R_s}{L_s} \\ A14 &= -\frac{\lambda_m}{L_s} F(\theta_e) \\ A24 &= -\frac{\lambda_m}{L_s} F\left(\theta_e + \frac{4\pi}{3}\right) \\ A34 &= -\frac{\lambda_m}{L_s} F\left(\theta_e - \frac{4\pi}{3}\right) \\ A41 &= \frac{\lambda_m}{J} G(\theta_e) \\ A42 &= \frac{\lambda_m}{J} G\left(\theta_e + \frac{4\pi}{3}\right) \\ A43 &= \frac{\lambda_m}{J} G\left(\theta_e - \frac{4\pi}{3}\right) \\ A44 &= -\frac{B}{J} \\ B11 &= B22 = B33 = \frac{1}{L_s} \\ B44 &= \frac{1}{J} \end{aligned}$$

where  $V_a$  is the phase  $a$  terminal voltage, the phase resistance, the phase current and the phase inductance are  $R_s$ ,  $i_a$ , and  $L_s$ , respectively. In particular, for phase  $b$  and  $c$ , we have similar voltage equations.  $J$  is inertia,  $B$  is friction coefficient,  $T_m$  is load torque, and  $\omega_m$  is magnet flux linkage of the stator winding. The nonlinear function  $G(\theta)$  can be described as follows:

$$G(\theta) = \begin{cases} \frac{6}{\pi} \theta & 0 < \theta \leq \frac{\pi}{6} \\ 1 & \frac{\pi}{6} < \theta \leq \frac{5\pi}{6} \\ -\frac{6}{\pi}(\theta - \pi) & \frac{5\pi}{6} < \theta \leq \frac{7\pi}{6} \\ -1 & \frac{7\pi}{6} < \theta \leq \frac{11\pi}{6} \\ \frac{6}{\pi}(\theta - 2\pi) & \frac{11\pi}{6} < \theta \leq 2\pi \end{cases} \quad (2)$$

The main idea of an estimation system in sensorless mode is to use a mathematical model derived from the BLDC to calculate the estimated value of the output parameters from the measured input parameters. Figure 1 shows the system operation block diagram of a BLDC sensorless speed control motor using estimator. The extended Kalman filter (EKF) is one type of common estimator, which is used to estimate the BLDC motor's system state variables and stator resistance immediately using the actual voltages and currents derived from the BLDC motor's mathematical model. In some cases, there is likewise some constraint in using EKF as an observer, for example, the characteristics of EKF that must be executed as first request accuracy, high multifaceted computing to calculate the Jacobian matrix and its covariance matrix.

For example in equation (1), mathematic model of the BLDC motor need  $T_m$  as input whereas, in reality, this load ( $T_m$ ) can not be measured directly. Meanwhile, in sensorless mode, the algorithm involves only the voltage and current BLDC motor terminals and does not involve any  $T_m$ , thus, if there is any  $T_m$ , it can cause an error of the estimate because one of the input is ignored. Figure 2 shows the estimation error. In two seconds, the load changes from 0 to 2 Nm and it can be seen that the estimation experiences an error. Therefore, we proposed the

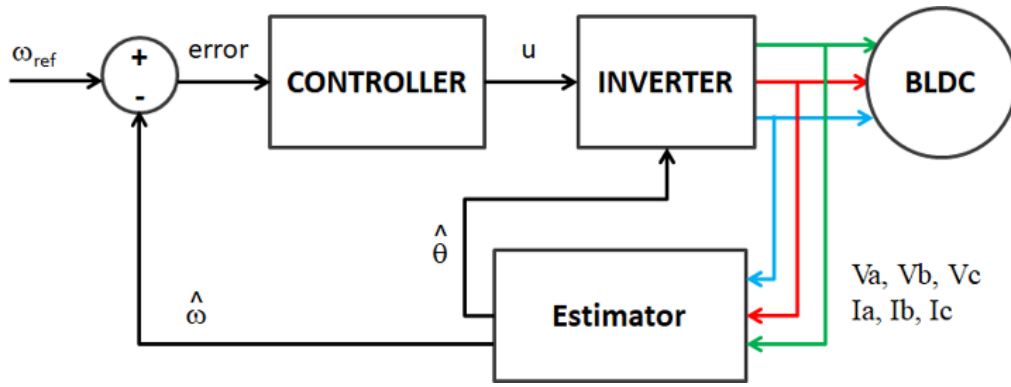


Figure 1. Block diagram of sensorless BLDC motor

EnKF and neural network algorithm as part of predicting the amount of  $T_m$  by changes in voltage and current that occurs in this paper.

### B. EnKF and neural network algorithm

Figure 3 shows the EnKF and neural network block diagram of the framework activity of a speed control sensorless BLDC motor. The EnKF as an estimator reckons, the rotor speed ( $\omega$ ) and the rotor position ( $\theta$ ). The rotor speed ( $\omega$ ), which is in a sensorless system is provided from the estimator and compared with the speed reference ( $\omega_{ref}$ ) to produce the speed error signal ( $e$ ). The resulting error is given to the controller. The controller will calculate this speed error signal ( $e$ ) into a control command ( $u$ ). Then, the voltage and current generated by the inverter is measured and used as input to block the neural network (NN) to estimate the  $T_m$ . Afterwards, the measured voltage and current and the estimated  $T_m$  resulted from the neural network are used as input to EnKF which ultimately results in the prediction of motor position and speed.

#### 1) Ensemble Kalman filter

The EnKF estimation system uses ensemble integration methods to solve the Fokker-Planck equation or also referred to as suboptimal where error statistics are predicted using Monte Carlo. In updating the filter gain  $\hat{K}_k$ , the EnKF system does not involve estimating nonlinear functions  $f(x, u)$  and

$h(x)$ . This is what distinguishes the EKF system in general, so that large computation in calculating the Jacobians of  $f(x, u)$  and  $h(x)$  is not used anymore in the EnKF system. The beginning stage for the EnKF estimation system as particle filters is the selection of a set of sample points, which is an ensemble of state estimations that captures the initial probability distribution of the state. These state estimation points are then engendered through the true nonlinear system, with the goal that the likelihood density function of the actual state can be approximated by the ensemble of the estimation system (EnKF).

The EnKF estimation method consists of three stages. The first step is called the forecast step, where the representation of the system's error statistics is gained by assuming that an ensemble of  $q$  forecast state estimates with random sample errors is available at time  $k$ . We denote this ensemble as  $X_k^f \in R^{n \times q}$  where

$$X_k^f \triangleq (x_k^{f_1}, x_k^{f_2}, \dots, x_k^{f_q}) \tag{3}$$

with the subscript  $f_i$  refers to the  $i$ -th forecast ensemble member. Then, the ensemble mean  $\bar{x}_k^f \in R^n$  is defined by

$$\bar{x}_k^f \triangleq \frac{1}{q} \sum_{i=1}^q x_k^{f_i} \tag{4}$$

Since the true state  $x_k$  is unknown, we approximate (4) by using the ensemble members. We define the

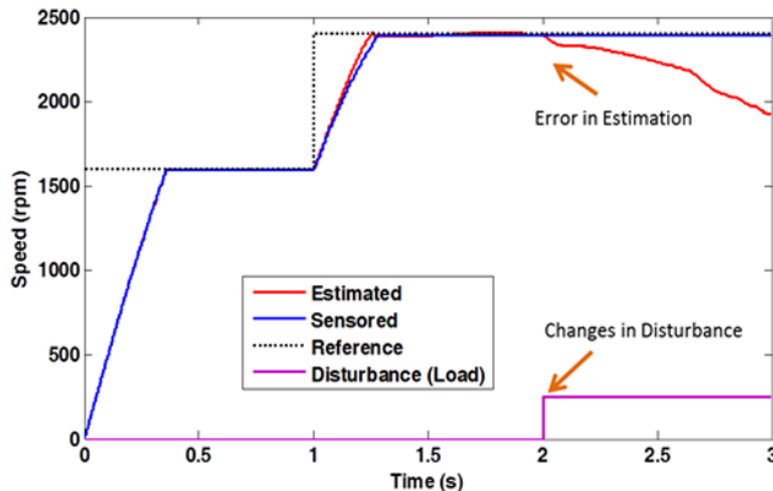


Figure 2. Performance curves of speed and load change before using neural network

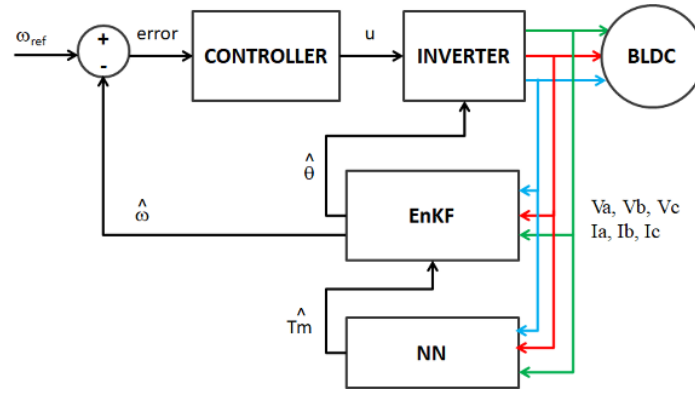


Figure 3. Block diagram of EnKF - neural network sensorless BLDCM

ensemble error matrix  $E_k^f \in R^{n \times q}$  around the ensemble mean by

$$E_k^f \triangleq [x_k^{f1} - \bar{x}_k^f \cdots x_k^{fq} - \bar{x}_k^f] \quad (5)$$

and the ensemble of the output error  $E_{y_k}^a \in R^{p \times q}$  by

$$E_{y_k}^a \triangleq [y_k^{f1} - \bar{y}_k^f \cdots y_k^{fq} - \bar{y}_k^f] \quad (6)$$

We approximate the  $P_k^f$  by  $\hat{P}_k^f$ , the  $P_{xy_k}^f$  by  $\hat{P}_{xy_k}^f$ , and the  $P_{yy_k}^f$  by  $\hat{P}_{yy_k}^f$ , respectively, where

$$\hat{P}_k^f \triangleq \frac{1}{q-1} E_k^f (E_k^f)^T, \hat{P}_{xy_k}^f \triangleq \frac{1}{q-1} E_{xy_k}^f (E_{xy_k}^f)^T \quad (7)$$

Therefore, we construe the forecast ensemble as the best forecast estimation of the state, while the distribution of the ensemble members around the average as the fault between the best estimation and the actual state. The second step is the analysis step. The EnKF carries out an ensemble of  $q$  parallel data assimilation cycles to obtain the state's analysis estimation, where for  $i = 1, 2, 3, \dots, q$

$$x_k^{ai} = x_k^{fi} + \hat{K}_k (y_k^i - h(x_k^{fi})) \quad (8)$$

The perturbed observations  $y_k^i$  are given by

$$y_k^i = y_k + v_k^i \quad (9)$$

where  $v_k^i$  is a zero-mean disordered variable with a normal distribution and covariance  $R_k$ . The sample fault of the covariance matrix computed from the  $v_k^i$  converges to  $R_k$  as  $q \rightarrow \infty$ . We approximate the analysis of the fault of the covariance matrices  $P_k^a$  by  $\hat{P}_k^a$ , where

$$\hat{P}_k^a \triangleq \frac{1}{q-1} E_k^a E_k^{aT} \quad (10)$$

And  $E_k^a$  is defined by with  $x_k^{fi}$  replaced by  $x_k^{ai}$  and  $\bar{x}_k^f$  replaced by the mean of the analysis estimate ensemble members. We use the classical Kalman filter gain expression and the approximations of the error covariances to determine the filter gain by  $\hat{K}_k$  by

$$x_{k+1}^{fi} = f(x_k^{ai}, u_k) + w_k^i \quad (11)$$

The last step is the prediction of error statistics in the forecast step:

$$x_{k+1}^{fi} = f(x_k^{ai}, u_k) + w_k^i \quad (12)$$

where the values are  $w_k^i$  sampled from a normal distribution with average zero and covariance  $Q_k$ . The

sample error covariance matrix computed from the  $w_k^i$  converges to  $Q_k$  as  $q \rightarrow \infty$ . Finally, we summarize the analysis and forecast steps.

Analysis steps were included equation (13) to equation (15).

$$\hat{K}_k = \hat{P}_{xy_k}^f (\hat{P}_{yy_k}^f)^{-1} \quad (13)$$

$$x_k^{ai} = x_k^{fi} + \hat{K}_k (y_k^i - h(x_k^{fi})) \quad (14)$$

$$\bar{x}_k^a = \frac{1}{q} \sum_{i=1}^q x_k^{ai} \quad (15)$$

Forecast steps were included equation (16) to equation (20).

$$x_{k+1}^{fi} = f(x_k^{ai}, u_k) + w_k^i \quad (16)$$

$$\bar{x}_{k+1}^f = \frac{1}{q} \sum_{i=1}^q x_{k+1}^{fi} \quad (17)$$

$$E_{k+1}^f = [x_{k+1}^{f1} - \bar{x}_{k+1}^f \cdots x_{k+1}^{fq} - \bar{x}_{k+1}^f] \quad (18)$$

$$E_{y_k}^a \triangleq [y_k^f - \bar{y}_k^f \cdots y_k^{fq} - \bar{y}_k^f] \quad (19)$$

$$\hat{P}_{xy_k}^f = \frac{1}{q-1} E_{xy_k}^f (E_{xy_k}^f)^T, \hat{P}_{yy_k}^f = \frac{1}{q-1} E_{yy_k}^f (E_{yy_k}^f)^T \quad (20)$$

## 2) Neural-network algorithm

The new modelling tool for a very well-known estimate is artificial neural networks, specifically used for complex and non-linear systems. Artificial neural networks do not require knowledge of the internal work processes of the system to be modelled so that they are usually used as black box models. But they only need learning from the input-output vectors produced by the experiment which are commonly called learning sets and represent the system for the model. Rumelhart proposed a back propagation learning method for the neural network learning process [17]. In this method, errors from the output of neural networks to learning data are formed into error functions and processed to a minimum. In the process of minimizing the function of this error, network parameters are updated with the principle opposite to the error function gradient.

In this paper, we use various load as inputs and current and voltage as outputs for data learning set. Figure 4 shows the neural network test result. This figure clearly shows that the estimated value of the neural network is in accordance with the actual value of the mean-sum-error (MSE) is  $5.7311 \times 10^{-5}$ .

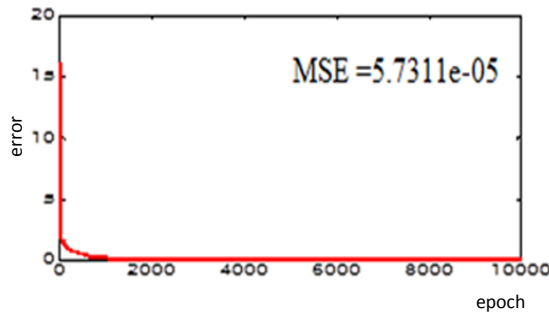


Figure 4. Performance of the neural network

### III. Results and Discussions

In this section, we present a sensorless velocity estimation and control system and simulation using MATLAB. The parameters of the BLDC motor are set with the following parameter, i.e. the stator resistance  $R_s = 79 \Omega$ , the inductance of the stator  $L_s = 12 \times 10^{-3} \text{ H}$ , each permanent magnet flux maximum phase winding  $\phi_m = 0.0271 \text{ Wb}$ , the inertia  $J = 0.48 \times 10^{-3} \text{ kg.m}^2$ , the viscous friction coefficient  $B_v$  is zero, poles of the permanent magnet  $p = 4$ , rated-torque  $0.125 \text{ Nm}$ , simulation step length  $T = 1 \times 10^{-4} \text{ s}$ ,  $x_0 = [0 \ 0 \ 0 \ 0]^T$  and number of ensemble is 10. Based on mathematical Equation (1) to get the prediction  $\omega$ , the

data needed are  $i_a, i_b, i_c, \omega, v_a, v_b, v_c$ , and  $T_m$  at the previous time.

The prediction process is done by using the EnKF algorithm. In this case,  $i_a, i_b, i_c, v_a, v_b$ , and  $v_c$ , are obtained from direct measurements and quickly sampling 10 times to get 10 ensembles, while  $\omega$  is the initial position and  $T_m$  is the estimated result of the neural network part. To substantiate the estimated performance of our algorithm, two treatments are performed to verify the performance of the velocity and the modification load.

In this example, the reference speed modifies from 1600 rpm to 2400 rpm at time  $t = 1 \text{ s}$ . Then, the load torque  $T_m = 0.07 \text{ Nm}$  is added to this motor at

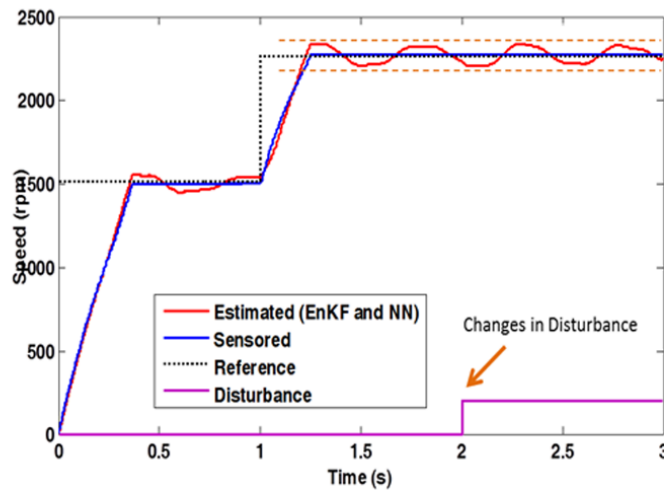


Figure 5. Performance curves of speed and load change after using neural network

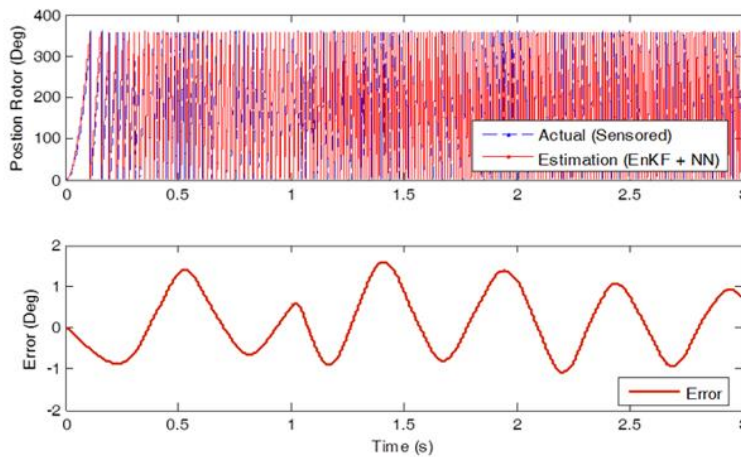


Figure 6. Performance of rotor position of speed and load change

time  $t = 2$  s. The experiment results (i.e. the performance curves) are obtained and presented in Figure 5 and Figure 6. From Figure 5, we can see that when the reference speed become different or the load become different, the evaluated and the real speed are nearly the same. The error between the estimated speed and the actual rate is approximately 3 %.

The ripple cannot be eliminated due to the interaction of the estimated EnKF and neural network but within an acceptable tolerance of 3 %. The designed EnKF and neural network algorithm can be concluded that it is very effective when the speed or torque changes suddenly. From Figure 6, it can be seen the evaluated and the real rotor position are almost identical. And the error is approximately 2 electrical angle confirming that the motor can operate normally with a small torque ripple. The results of the experiments show the efficacy of our filtering algorithm.

## Conclusion

In this paper, to operate a sensorless BLDC motor, we developed a new estimation system for rotor speed and rotor position speed using an ensemble Kalman filter (EnKF) and neural network. It is clear that the precise estimation performance can be obtained from the simulation results and the efficiency of our designed algorithm can be illustrated. With a disturbance of 50 % of the rated-torque, the proposed algorithm is able to maintain motor speed with a speed error of 3 % and error estimated position is approximately 2 electrical angle. Additionally, the sensorless BLDC motor can also be precisely controlled according to the designed algorithm of EnKF and neural network.

## Acknowledgement

The authors would like to thank all members of Computational Intelligence and Intelligent System, Department of Electrical Engineering, Universitas Indonesia, which have already supported the research. The valuable comments from the reviewers are also very much appreciated.

## Declarations

### Author contribution

All authors contributed equally as the main contributor of this paper. All authors read and approved the final paper.

### Funding statement

This research did not receive any specific grant from funding agencies in the public, commercial, or not-for-profit sectors.

### Conflict of interest

The authors declare no conflict of interest.

### Additional information

No additional information is available for this paper.

## References

- [1] A. Ulasayar, H. Sheh Zad and A. Zohaib, "Intelligent Speed Controller Design for Brushless DC Motor," *2018 International Conference on Frontiers of Information Technology (FIT)*, Islamabad, Pakistan, pp. 19-23, 2018.
- [2] L. Chu *et al.*, "Research on Control Strategies of an Open-End Winding Permanent Magnet Synchronous Driving Motor (OW-PMSM)-Equipped Dual Inverter with a Switchable Winding Mode for Electric Vehicles," *Energies*, vol. 10, no. 5, pp. 616, 2017.
- [3] J. H. R. Bo Long, Shin Teak Lim, and K. T. Chong, "Energy-Regenerative Braking Control of Electric Vehicles Using Three-Phase Brushless Direct-Current Motors," *Energies*, vol. 7, pp. 99–114, 2014.
- [4] S. A. KH. Mozaffari Niapour, M. Tabarraie, and M. R. Feyzi, "A new robust speed-sensorless control strategy for high-performance brushless DC motor drives with reduced torque ripple," *Control Engineering Practice*, Volume 24, Pages 42-54, 2014.
- [5] O. Imoru and J. Tsado, "Modelling of an electronically commutated (Brushless DC) motor drives with back-emf sensing," *2012 16th IEEE Mediterranean Electrotechnical Conference*, Yasmine Hammamet, pp. 828-831, 2012.
- [6] M. Mariano, K. Scicluna, and J. Scerri, "Modelling of a sensorless rotor Flux oriented BLDC machine," *2017 19th International Conference on Electrical Drives and Power Electronics (EDPE)*, Dubrovnik, pp. 194-199, 2017.
- [7] C. S. Joice, S. R. Paranjothi and V. J. S. Kumar, "Digital Control Strategy for Four Quadrant Operation of Three Phase BLDC Motor With Load Variations," in *IEEE Transactions on Industrial Informatics*, vol. 9, no. 2, pp. 974-982, 2013.
- [8] G. Liu *et al.*, "Sensorless Control for High-Speed Brushless DC Motor Based on the Line-to-Line Back EMF," in *IEEE Transactions on Power Electronics*, vol. 31, no. 7, pp. 4669-4683, 2016.
- [9] T. W. Chun *et al.*, "Sensorless control of BLDC motor drive for an automotive fuel pump using a hysteresis comparator," *IEEE Trans. Power Electron.*, vol. 29, no. 3, pp. 1382–1391, 2014.
- [10] G. J. Su and J. W. McKeever, "Low-cost sensorless control of brushless DC motors with improved speed range," *IEEE Trans. Power Electron.*, vol. 19, no.2, pp. 296–302, 2004.
- [11] Y. Y. Wu *et al.*, "Position sensorless control based on coordinate transformation for brushless DC motor drives," *IEEE Trans. Power Electron.*, vol. 25, no. 9, pp. 2365–2371, 2010. R. M. Pindoriya *et al.*, "FPGA Based Digital Control Technique for BLDC Motor Drive," *2018 IEEE Power & Energy Society General Meeting (PESGM)*, Portland, OR, pp. 1-5, 2018.
- [12] R. M. Pindoriya, A. K. Mishra, B. S. Rajpurohit and R. Kumar, "FPGA Based Digital Control Technique for BLDC Motor Drive," *2018 IEEE Power & Energy Society General Meeting (PESGM)*, Portland, OR, pp. 1-5, 2018.
- [13] U. K. Soni and R. K. Tripathi, "Novel back EMF zero difference point detection based sensorless technique for BLDC motor," *2017 IEEE International Conference on Industrial Technology (ICIT)*, Toronto, ON, pp. 330-335, 2017.
- [14] Tae-Hyung Kim, Hyung-Woo Lee, and M. Ehsani, "State of the art and future trends in position sensorless brushless DC motor/generator drives, Industrial Electronics Society," *IECON 2005. 31st Annual Conference of IEEE*, pp.8, 6-10 Nov., 2005.
- [15] M. Rif'an, F. Yusivar, and B. Kusumoputro, "Design of Extended Kalman Filter Speed Estimator and Single Neuron-Fuzzy Speed Controller for Sensorless Brushless DC Motor," *Journal of Telecommunication, Electronic and Computer Engineering (JTEC)*, Vol. 10, No. 1-5, 2018.
- [16] M. Rif'an, F. Yusivar, and B. Kusumoputro. "Estimation and Control of Sensorless Brushless DC Motor Drive using Ensemble Kalman Filter." In *Proceedings of the 8th International Conference on Computer Modeling and Simulation (ICCMS 17)*. ACM, New York, USA, pp. 192-195, 2017.
- [17] D. E. Rumelhart and J. L. McClelland, "Explorations in the microstructure of cognition. Parallel distributed processing Chap. 8," MIT Press Cambridge, USA., 1986.